Modeling and Motion Control of a Soft Robot

Yanqiong Fei and Hongwei Xu

***Abstract*—A soft robot with locomotive abilities controlled by body deformations is modeled, analyzed, and then constructed in this study. The robot is composed of a thin steel shell, four sensors, and four shape memory alloy (SMA) springs. Due to the force exerted by the SMAs, the thin steel shell deforms and causes the robot to roll and move forward continuously. The study is conducted in four tiers. Initially, after producing a model of the soft robot, the constraint conditions of rolling actions from deformations are analyzed. Then, the relationship between the deformation and the heating time of SMAs is studied. A dynamic analysis on the rolling motion is presented based on the deformation of SMAs and the change in the robot's center of gravity. A dynamic simulation is also conducted to test the feasibility of the theory. The third tier consists of designing a closed-loop controller based on feedback data from the four deformable sensors, a feature that has never been applied to soft robots in previous studies. Finally, a prototype of the soft robot is built, and an experiment is conducted and compared to prove the validity of the theory.**

***Index Terms*—Deformation, feedback, roll, soft robot.**

I. Introduction

TRADITIONAL mobile robots consist of hard and rigid components. Their most important advantage is the convenience of accurately controlling and detecting the positions, poses, and actions. However, robots that contain rigid structures have several crucial shortcomings, such as not adapting to environments of high complication, and the complicated control of carrying fragile objects smoothly [1]. Thus, robots with soft bodies are produced to overcome these limitations [2], [3]. Soft robotics is expected to play an important role in establishing substantially novel approaches and applications in robotic research. Soft robots have many advantages and priorities compared to traditional rigid robots. One of their main characteristics is their low resistance to stress forces. Like caterpillars, they can morph between different shapes to move, their size and shape can be also altered over a large range, which has potential applications in detection, exploration, succor, and medicine. Another advantage is that they can safely interact with humans and natural environments [4]. Previous studies suggest that these robots are efficient in mimicking the motions of natural living creatures, which could allow them to adapt to various environments [5], [6]. Rather than moving via wheels, legs, or caterpillar bands generally equipped in rigid robotics, soft robots usually move through the deformation of their soft structures. Several researchers have successfully constructed robots of soft body type, yet their motions are limited. Amend invented a grasper consisting of a flexible sac filled of granular materials, which could grip objects of various sizes and shapes, by controlling vacuum pressure within the robot structure [7]. In another study, Robert *et al.* presented a soft walker that was actuated by compressing air [8]. Seok *et al.* invented a worm robot that accomplished peristaltic locomotion by shrinking its compliance mesh made body [9]. Fei *et al.* presented a kind of soft robot composed of several spherical cells that could deform individually, contributing to the robot's motion [10], [11].

Shape memory alloys (SMAs) are becoming a commonly used material in soft robotics. For instance, Margheri *et al.* designed an octopus-like robot with artificial muscles made of SMA springs arranged longitudinally and transversely [12], [13]. When actuated, the SMA springs generated force within the robot's body, which led to deformations, including elongation, shortening, bending, and stiffening. Similarly, Sugiyama and Hirai designed a circular rubber shell robot driven by SMA coils that can crawl and jump via deformations [14]. However, due to the rubber shell, the robot cannot work with heavy loads. Because the characteristics of different SMA springs are not identical, it is easy for the connection of the eight coils to deviate from the center of the gravity in the robot. It is also difficult to produce continuous motion of the circular rubber shell.

In this paper, we design a prototype of a soft robot. The material of the shell is replaced by thin deformable steel, which allows it to work with heavy loads. In order to ensure deformation uniformity in every direction, four SMA springs are arranged along the diameter direction instead of along the radial direction. To achieve automatic and continuous locomotion, four sensors are pasted on the inside surface of the thin shell. A closed-loop controller is built, a feature that has never been considered in the field of soft robotics. A model theory of the robot is presented and a physical simulation performs to validate our motion analyses and theory. We then perform the experiment after constructing a prototype of the soft robot based off the model. The results of the physical prototype are in agreement with the predictions made from the theoretical analysis and simulations.

II. Structure of the Soft Robot

The robot is built with a circular thin steel shell, four SMA springs, four sensors, and a control system. The four SMA springs are arranged along the diameter direction as to divide

Manuscript received November 30, 2015; revised March 4, 2016; accepted April 5, 2016. Date of publication May 24, 2016; date of current version January 10, 2017. This work was supported in part by the National Natural Science Foundation of China under Grant 51475300 and in part by the Open Foundation of First Level Zhejiang Key in Key Discipline of Control Science and Engineering.

Y. Fei is with the Institution of Robotics, Shanghai Jiaotong University, Shanghai 200240, China, and also with the School of Automation, Hangzhou Dianzi University, Hangzhou 310018, China (e-mail: fyq@sjtu.edu.cn).

H. Xu is with the Institution of Robotics, Shanghai Jiaotong University, Shanghai 200240, China (e-mail: xuhongwei@sjtu.edu.cn).

Color versions of one or more of the figures in this paper are available online at http://ieeexplore.ieee.org.

Digital Object Identifier 10.1109/TIE.2016.2572670

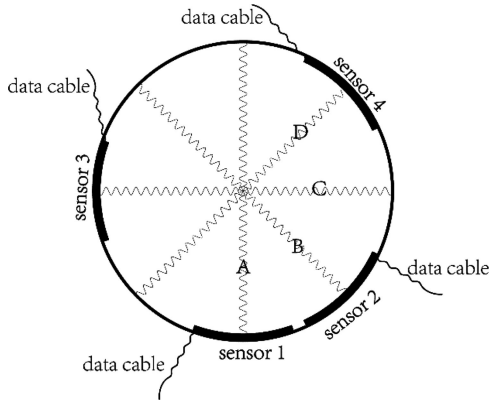

Fig. 1. Structure of the soft robot.

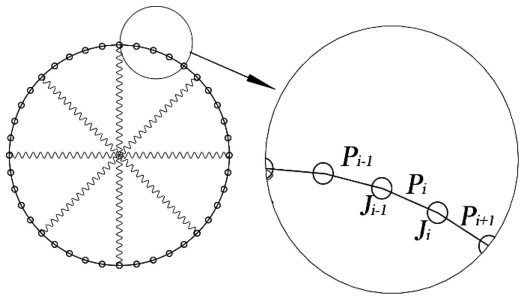

Fig. 2. Model of the soft robot.

the thin steel shell into eight equivalent parts. The SMA springs are labeled A, B, C, and D, as shown in Fig. 1. The sensors are then pasted on the inside surface of the thin shell. They are specially positioned to balance the influence of the data cables, while ensuring that all SMA springs could be detected. In order to investigate the deformation of the robot, we assume that the shell consists of 40 parts ($P_i = 1, 2, \ldots, 40$), as shown in Fig. 2. The value 40 is obtained after modifications. After several simulations, 40 parts will not cause considerable error and the simulation will be achieved within an acceptable time.

III. Modeling of the Circular Thin Shell

According to the beam bending theory, a beam will bend and generate moments in its cross sections. The deformation is determined from the forces and moments applied to the soft robot as well as the material property of the beam.

The circular thin shell of the robot is divided into 40 portions, as seen in Fig. 2. The sensors are light enough to ignore. Each region is assumed to consist of three sequential portions P_{i-1}, P_i, P_{i+1}. The relationship between deformation and the forces as well as moments applied to the system is illustrated in Fig. 3.

The deformations are represented by the curvatures of all cross sections of the shell, and the curvatures of every cross section are represented by the angle between the two portions near the cross section, where P_i is a portion of the shell, and P_{i-1}, P_{i+1} are its neighboring portions. M_{i-1} and M_i are the moments applied to the beam between the two adjacent portions, and ρ_{i-1} and ρ_i are the radii of curvature in two neighboring

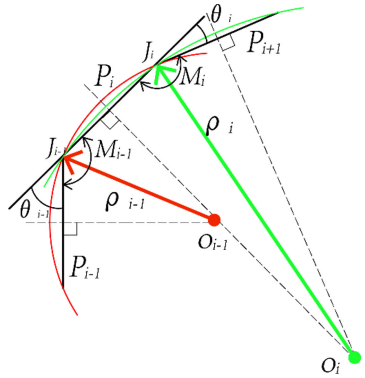

Fig. 3. Deformation model of the shell.

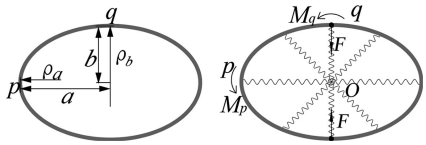

Fig. 4. Force and moment model.

deformation areas. J_{i-1} and J_i are two joints. o_{i-1} and o_i are the centers of curvature in J_{i-1} and J_i, respectively. θ_{i-1} and θ_i are the acute angles between P_{i-1} and P_i, respectively, as well as P_i and P_{i+1}.

According to Fig. 3,

$$\rho_i = (L/2) / \left[\cos^{-1}\left((\pi - \theta_i)/2\right)\right] \tag{1}$$

where L is the length of every portion, it can be obtained that

$$L = \pi r/20 \tag{2}$$

where r is the radius of the circular shell.

As described in Fig. 3, the model of deformation is described by the following equation:

$$M_i = EI_z/\rho_i. \tag{3}$$

According to the above equations, the relationship between θ_i and M_i can be described as follows:

$$\theta_i = \pi - 2 \cdot \cos^{-1}\left(3M_i\pi r/10Evw^3\right) \tag{4}$$

where E is the elasticity modulus of the shell. I_z is the moment of inertial of the cross section to the neutral axis. v is the thickness of the shell, and w is its width.

IV. Modeling on the Deformation and Heating Times of SMA Springs

In the original state, the radius of the robot's shell is *r*, and the center of the robot's shell is *o*. In the deformable state, the long radius *op* is *a*, and the short radius *oq* is *b*, as seen in Fig. 4. The perimeter *l* is

$$l = 2\pi b + 4(a - b). \tag{5}$$

Here,

$$a = (\pi r - \pi b + 2b)/2. \tag{6}$$

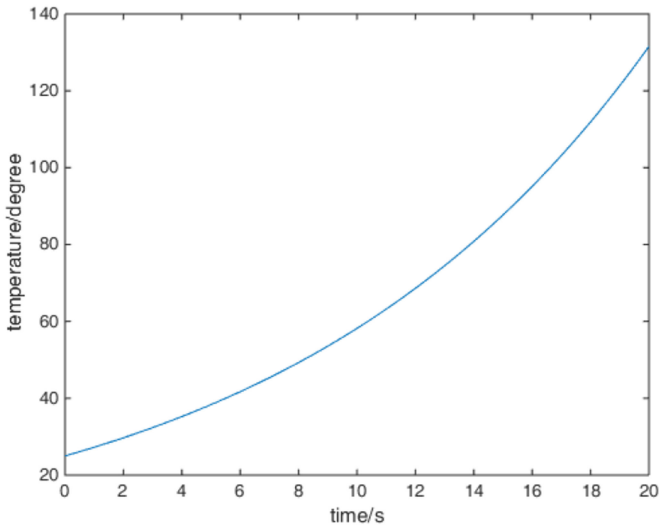

Fig. 5. Relationship between *T* and *t*.

The deformation of SMA spring is δ.

$$\delta = 2(r-b). \tag{7}$$

The moments on p, q are

$$M_p = EI_Z/\rho_p \tag{8}$$

$$M_q = EI_Z/\rho_q. \tag{9}$$

Here,

$$\rho_p = b^2/a \tag{10}$$

$$\rho_q = a^2/b \tag{11}$$

$$M_p - M_q = Fa. \tag{12}$$

We can obtain

$$F = 4EI_Z/(2r-\delta)^2 - EI_Z \times (8r-4\delta)/(\pi\delta/2+2r-\delta)^3. \tag{13}$$

Here, *F* is the force on one SMA spring. We can obtain the relationship between the force *F*, temperature *T*, and deformation δ of one SMA spring [15]

$$F = \pi d^3/(8D)\tau(\delta,T) = \pi d^3/(8D)\left\{\tau(0,T_0) + [A\delta d/(n\pi D^2) + B(T-T_0)]\sum_{i=0}^{\infty} C_i\delta^i\left(d/(n\pi D^2)\right)^i\right\}. \tag{14}$$

Here, $\tau(0,T_0) = 0$. *D* is the outer diameter of the SMA spring. *d* is the inner diameter of the SMA spring. A, B, C_i are material parameters that are obtained from experimental data.

Thus, when the deformation δ is known, the temperature *T* can be obtained

$$T = \{F/\left[\sum_{i=0}^{\infty} C_i\delta^i(d/(n\pi D^2))^i\right] - A\delta d/(n\pi D^2)\}/B + T_0. \tag{15}$$

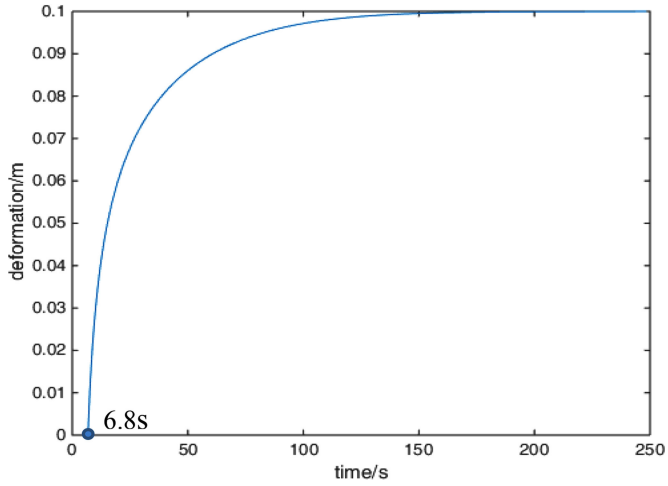

Fig. 6. Curve of the deformation δ and the heating time *t*.

The thermal equilibrium equation [16] of the SMA spring is

$$U^2/R - mc\,dT/dt = -hA_s(T-T_f). \tag{16}$$

From (16), we can obtain

$$T = He^{thA_s/(mc)} - U^2/(RhA_s) + T_f. \tag{17}$$

Here, H is a constant. *U* is the voltage. *R* is the resistance of one SMA spring that is obtained from the experiment. A_s is the heating area. *m* is the quality of one SMA spring. T_f is the temperature of the environment. *h* is the coefficient of heating conduction. *C* is the specific heat capacity of SMA springs. *t* is the time of heating SMA spring.

From (17), the relationship between *T* and *t* is determined to be in Fig. 5

$$t = mc\cdot\ln\left(\left(T+U^2/(RhA_s)-T_f\right)/\mathrm{H}\right)/(hA_s). \tag{18}$$

Based on (15) and (18), the relationship between the deformation δ and the heating time *t* is shown in Fig. 6.

From Fig. 6, when the heating time *t* is less than 6.8 s, the deformation is zero. When the heating time is more than 6.8 s, the SMA spring begins to deform. When the diameter of the shell decreases close to 0.1 m, the SMA spring stops deforming.

V. Dynamic Analysis on Rolling

Based on the model of the circular shell and deformation of SMA springs, dynamic analysis on the robot movement is performed. A completed round roll consists of eight identical cycles, each of which has four steps, as illustrated in Fig. 7.

1) *Step 1:* The robot is in the original state and displays a circular shape. The point that the robot is in contact with the ground is denoted G_i.
2) *Step 2:* Spring B is actuated and shrinks. The point of contact shifts from deformations, and the next contact point is denoted G_j.

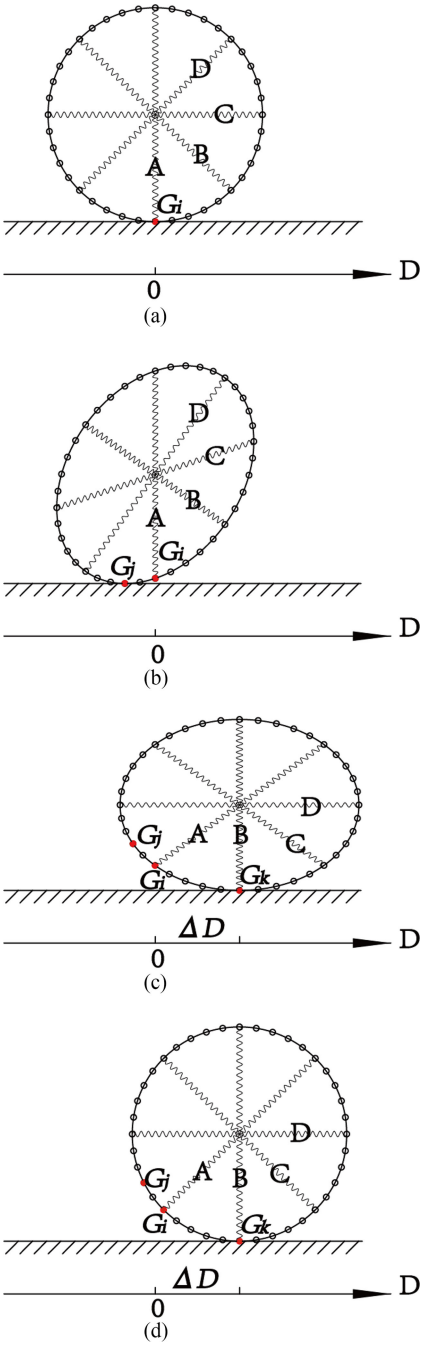

Fig. 7. Dynamic analysis of rolling.

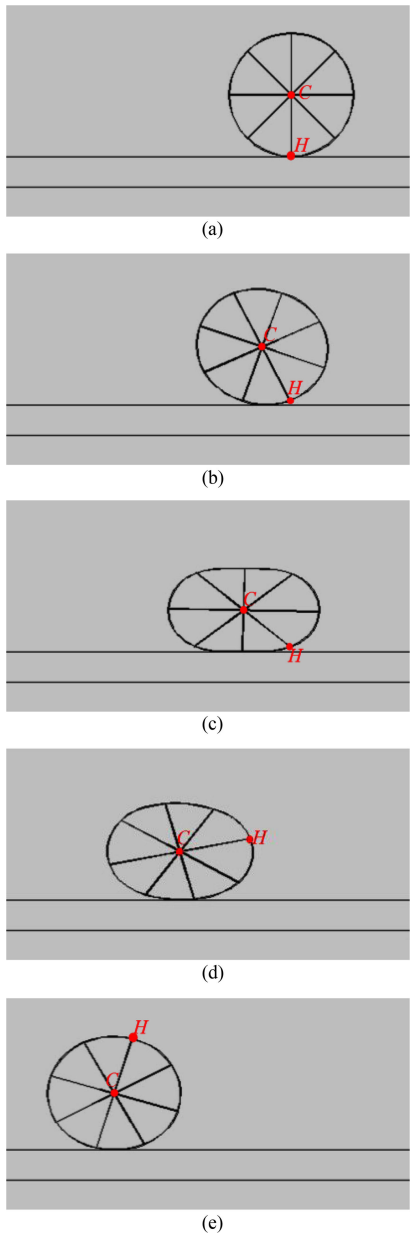

Fig. 8. Result of simulation. (a) 0 s, (b) 20 s, (c) 40 s, (d) 60 s, and (e) 80 s.

At the same time, a driving moment is applied to the robot via gravity and can be calculated by the following equation:

$$M_d = \sum_{l=1}^{40} \hat{m} g \left(x_l - x_i\right) / 40 \tag{19}$$

where $\hat{m}$ is the robot's mass; and $(x_l - x_i)$ is the horizontal distance between the contact points G_l and G_i. It is obvious that this is an unbalanced position. Because of the effect of M_d, the robot is able to roll on the ground.

3) *Step 3:* The robot obtains a new balanced position and rolls a short distance. The latest contact point is G_k. Also at this point, the robot stops actuating the spring B.

4) *Step 4:* Deformation disappears, and the shell becomes a circle again. The next cycle ensues, beginning back at Step 1. In an entire cycle, the robot covers a displacement $\Delta D = \pi r/4$.

VI. Motion Control With Four Sensors

In order to control the automatic rolling, a closed-loop controller is built.

Four curvature sensors (labeled sensor 1, sensor 2, sensor 3, and sensor 4) pasted inside the thin shell are able to detect changes in curvature. Each sensor is equally separated by a corresponding SMA spring, as can be seen in Fig. 1. The curvature sensor's resistance decreases as its curvature increases. The resistance of a sensor signals which SMA spring is

TABLE I
PARAMETERS OF THE ROBOT MODEL

Parameter	Value
v	0.3 mm
w	30 mm
R	100 mm
E	2×10^{11} Pa
ρ	7850 kg/(m^3)

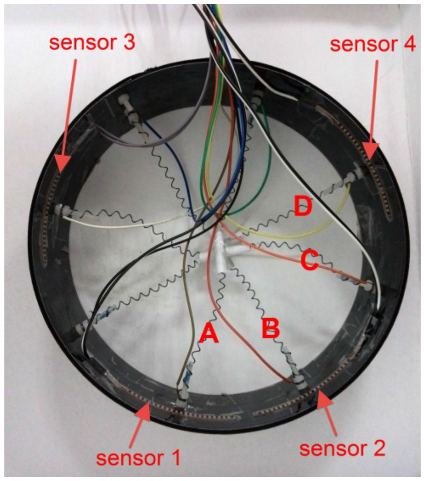

Fig. 9. Prototype of the robot.

actuated. From this, the information of the robot's deformation is obtained and used to control the rolling and forward motions.

At the beginning of a motion cycle, the shape of the robot's shell is circular. The sensors are in their original state, and their resistance is at the minimum value $R_{\min}$ and when the corresponding SMA spring achieves the most deformation, their resistance is at the maximum value $R_{\max}$. Their current resistance is R_i, which will obviously be in the range $[R_{\min},\ R_{\max}]$. After a 10-bits A/D conversion, the controller obtains the reading of a sensor. Thus, the deformation of the sensors can be evaluated by the following equation:

$$\Delta_i = (R_i - R_{\min}) / (R_{\max} - R_{\min}) \times 2^{10}\ (i = 1, 2, 3, 4)\,. \quad (20)$$

The change in curvature of each corresponding SMA spring, Δ_i, ranges from 0 to 1024. Based on the data from the sensors, the control system can deduce the robot's state and decide which spring to be actuated in the following step.

Initially, spring A is actuated and shrinks. When Δ_1 is detected larger than 800, it can be regarded that spring A has achieved its greatest deformation and is vertical to the horizon. If the robot is to roll clockwise, it stops heating spring A and begins to actuate spring B. When Δ_2 is larger than 800, the robot stops spring B's actuation and actuates spring C, until Δ_3 is larger than 800. Spring D is actuated in the next step, and when Δ_4 is larger than 800, the robot stops actuating spring D and begins to actuate spring A. Thus, with the feedback data, the process above is repeated, allowing the robot to roll continuously and automatically.

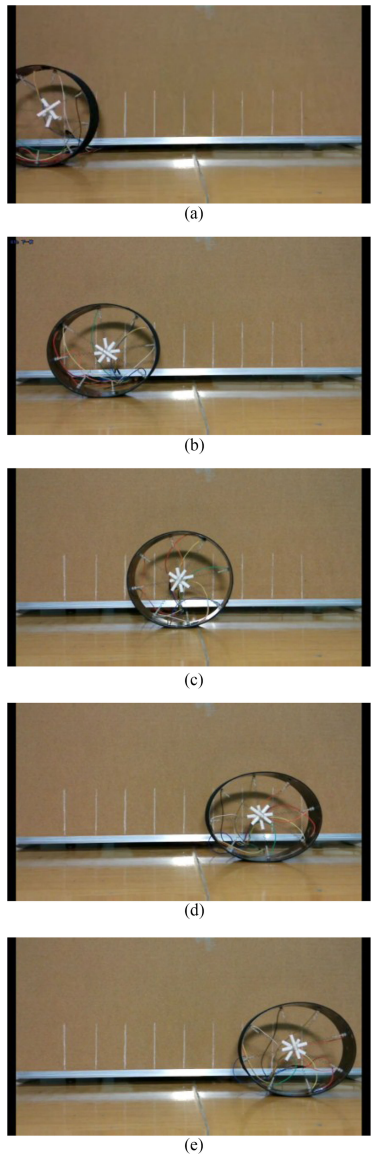

Fig. 10. Locomotion of the robot. (a) 0 s, (b) 20 s, (c) 40 s, (d) 60 s, and (e) 80 s.

VII. SIMULATION

Based on the model and analysis described above, the locomotion of the robot is simulated (see Fig. 8). All the simulation parameters match the prototype of the robot (see Table I).

In Fig. 8(a), the robot lies on the ground with no springs actuated. In Fig. 8(b), SMA spring A is actuated and begins to shrink, which leads to the deformation of the circular shell. Because of this deformation, the point where the shell contacts the ground moves to the right, relative to the robot's center of gravity, which generates a moment around the contacting points applied to the robot. Thus, the robot could twirl the contacting point, as shown in Fig. 8(c). When the SMA springs are periodically actuated in turns, the robot is able to roll on the ground.

VIII. EXPERIMENT

A prototype model of the robot is designed. The robot is composed of a circular thin shell, four SMA springs (A, B,

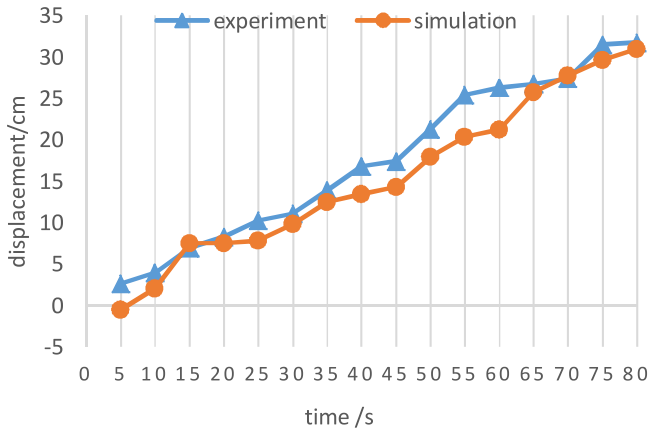

Fig. 11. Displacement of simulation and experiment.

C, D), four sensors, and a control system (see Fig. 9), and the power this robot consumes is less than 6 W. The SMA springs are equally placed along the diameter direction and connected to the shell by their endpoints. When the springs are electrified, heat is generated. Once the temperature of SMA springs increases past a threshold value, they shrink which deforms the shell and causes the soft robot to roll. In the experiment, the springs are actuated in turns periodically in a counterclockwise direction. Fig. 10 illustrates the process of the robot's locomotion. The robot is able to roll continuously on the ground and move forwards. It can be seen that the experimental results of the prototype fit the physical simulation well, which proves validity of the motion theory established prior to robot constructions. Fig. 11 shows the displacement of simulation and experiment in a period. We conclude that the experimental results of the prototype are in good agreement with the physical simulation, which further proves our theory's validity.

IX. Conclusion

In this paper, we have presented the construction and analysis of a soft robot that can move forward by controlling the deformation with the feedback data of SMAs. The robot is composed of a thin steel shell, four SMA springs, four sensors, in addition to a control system. Based on the geometric features, the constraint conditions of rolling actions with deformation were analyzed. We are able to model a relationship between the deformation and the heating time of SMAs with the thermal equilibrium equation of the SMA springs. A closed-loop controller is designed based on this relationship, and with the feedback data of four deformable sensors, a motion control method is described. After establishing theory of motion, a prototype of the soft robot was built and a simulation and an experiment are conducted to prove that the soft robot can roll and move forward. Based on our successful results, we believe this soft robot can adapt to different terrains. Its various ranges of deformation allow it to cross gaps smaller than itself; thus, it could carry out tasks (such as detection in a narrow environment) in places where humans cannot reach.

In further research, the control method will be improved and the control system integrated into the robot body should be designed and analyzed in order to understand and broaden its working scope and make it autonomous.

References

[1] S. Bauer, S. Bauer-Gogonea, I. Graz, M. Kaltenbrunner, C. Keplinger, and R. Schwödiauer, "25th anniversary article: A soft future: From robots and sensor skin to energy harvesters," *Adv. Mater.*, vol. 26, no. 1, pp. 149–162, Jan. 2014.

[2] I. Fumiya and C. Laschi, "Soft robotics: Challenges and perspectives," *Procedia Comput. Sci.*, vol. 7, pp. 99–102, 2011.

[3] B. Trimmer, "Soft robots," *Curr. Biol.*, vol. 23, no. 15, pp. R639–R641, 2013.

[4] S. Kim, C. Laschi, and B. Trimmer, "Soft robotics: A bioinspired evolution in robotics," *Trends Biotechnol.*, vol. 31, no. 5, pp. 287–294, May 2013.

[5] Y. Q. Fei and X. Y. Shen, "Nonlinear analysis on moving process of soft robots," *Nonlinear Dyn.*, vol. 73, nos. 1/2, pp. 672—677, Jul. 2013.

[6] B. Trimmer, H. Lin, B. Amanda, G. G. Leisk, and D. L. Kaplan, "Towards a biomorphic soft robot: Design constraints and solutions," in *Proc. IEEE RAS EMBS Int. Conf. Biomed. Robot. Biomechatron.*, Rome, Italy, Jun. 2012, pp. 599–605.

[7] J. Amend, B. Eric, R. Nicholas, and H. Jaeger, "A positive pressure universal gripper based on the jamming of granular material," *IEEE Trans. Robot.*, vol. 28, no. 2, pp. 341–350, Apr. 2012.

[8] R. F. Shepherd *et al.*, "Multigait soft robot," *Proc. Nat. Acad. Sci.*, vol. 108, no. 51, pp. 20400–20403, Dec. 2011.

[9] S. Seok, C. D. Onal, R. Wood, D. Rus, and S. Kim, "Peristaltic locomotion with antagonistic actuators in soft robotics," in *Proc. IEEE Int. Conf. Robot. Autom.*, Anchorage, AK, USA, May 3–7, 2010, pp. 1228–1233.

[10] Y. Q. Fei and H. W. Gao, "Nonlinear dynamic modeling on multi-spherical modular soft robots," *Nonlinear Dyn.*, vol. 78, no. 2, pp. 831–838, Oct. 2014.

[11] Y. Q. Fei and X. Wang, "Study on nonlinear obstacle avoidance on modular soft robots," *Nonlinear Dyn.*, vol. 82, pp. 891–898, Oct. 2015.

[12] L. Margheri, C. Laschi, and B. Mazzolai, "Soft robotic arm inspired by the octopus: I. From biological functions to artificial requirements," *Boinspir. Biomim.*, vol. 7, no. 2, pp. 25004–25015, May 2012.

[13] B. Mazzolai, L. Margheri, M. Cianchetti, P. Dario, and C. Laschi, "Soft-robotic arm inspired by the octopus: II. From artificial requirements to innovative technological solutions," *Bioinspir. Biomim.*, vol. 7, no. 2, pp. 25005–25005, May 2012.

[14] Y. Sugiyama and S. Hirai, "Crawling and jumping by a deformable robot," *Int. J. Robot. Res.*, vol. 25, nos. 5/6, pp. 603–620, May 2006.

[15] A. Chen and X. Qian, "Research on mechanical characteristics mathematical model of shape memory alloy spring," *Mach. Build. Autom.*, vol. 1, pp. 14–23, 1999.

[16] Y. L. Zhang, "The theory of structure and experimental research on SMA linear actuator," M.S. thesis, Dept. Electron. Eng., Univ. Science Technol. China, Hefei, China, 2010.

Yanqiong Fei received the M.Eng. degree from Southeast University, Jiangsu, China, in 1998, and the Ph.D. degree from Shanghai Jiaotong University, Shanghai, China, in 2002.

From September 2010 to September 2011, she was a Visiting Scholar with the Department of Mechanical Engineering, Massachusetts Institute of Technology, Cambridge, MA, USA. Since 2004, she has been an Associate Professor at the Research Institute of Robotics, Shanghai Jiaotong University. Her research interests include robotics, self-reconfigurable modular robots, and soft robots. She has published more than 80 paper three book chapters, and 20 patents in these areas.

Hongwei Xu was born in Baoding, China. He is currently working toward the M.Eng. degree at the Research Institute of Robotics, Shanghai Jiaotong University, Shanghai, China.

His main research interests include soft robots.